# Geomagnetic Secular Variation at Low Latitudes
## Observational Constraints and Theoretical Challenges


Chris Finlay

Institut für Geophysik, ETH Zürich


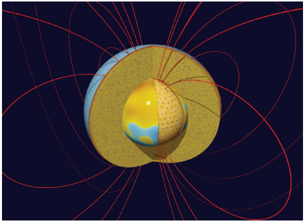

Seminar at DTU Space, Thurs 11th Nov 2010

# Talk Outline

1. **Introduction**
2. Historical field evolution
3. Monitoring today's geodynamo
4. Origin of field changes: Dynamics of the core
5. Future prospects and conclusions

# The Earth's magnetic field

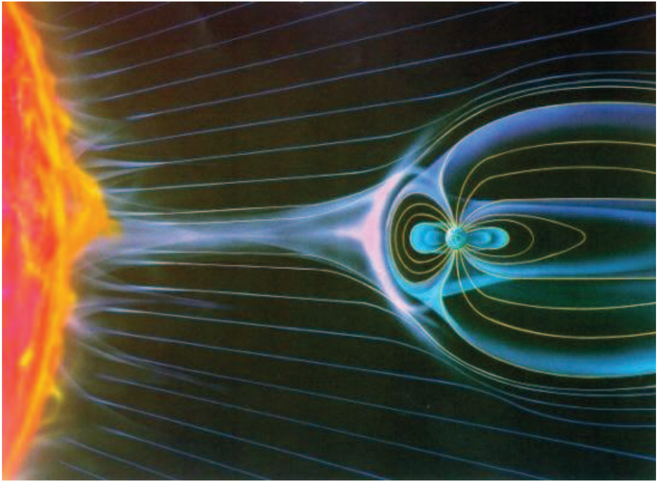

**Fig 1.1:** Schematic picture of Earth's magnetic field interacting with the solar wind(credit: NASA)

- Mediates between the Earth and the wider solar-system environment.

# Primary source - dynamo in our planet's core

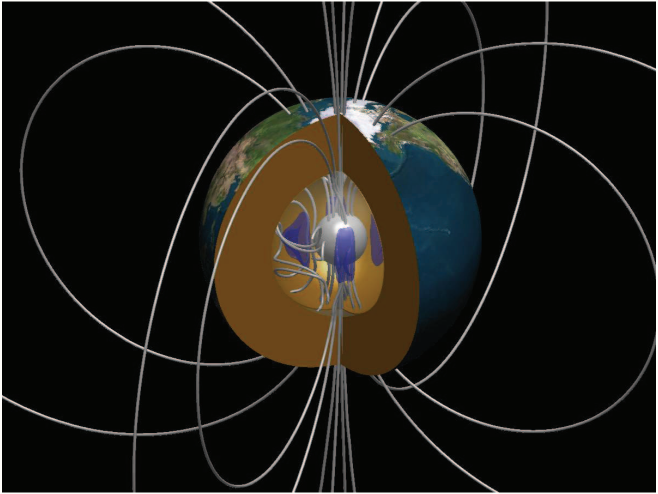

**Fig 1.2:** The geodynamo operating in Earth's core (credit: J. Aubert, IPGP)

- Thermochemical convection in Earth's core drives motions which generate electrical currents and sustain the geomagnetic field.

# Components of the geomagnetic field

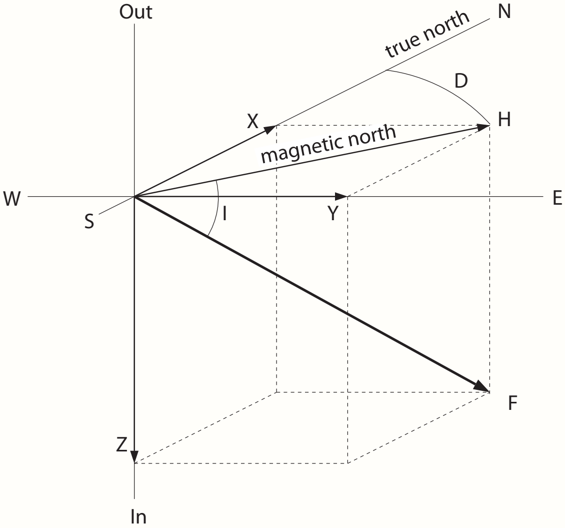


**Fig 1.3:** Components of the geomagnetic field.

# Practical applications: directional information

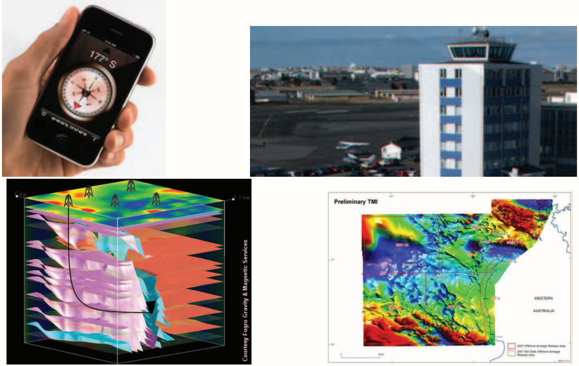


**Fig 1.4:** Mobile phones, Air traffic control, Directional drilling, Anomaly mapping.

- Use of electronic compasses now very widespead in mobile phones & compact cameras. Also for drill orientation in hydrocarbon industry.

# Practical applications: directional information

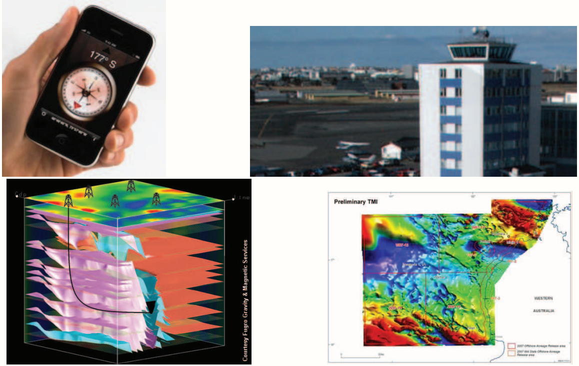


**Fig 1.4:** Mobile phones, Air traffic control, Directional drilling, Anomaly mapping.

- Use of electronic compasses now very widespead in mobile phones & compact cameras. Also for drill orientation in hydrocarbon industry.
- But requires an accurate model of the current geomagnetic field.

# Practical applications: directional information

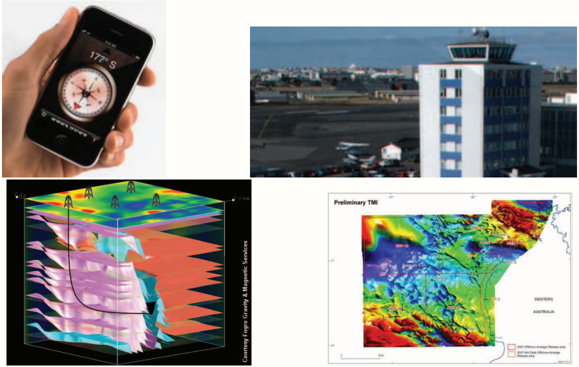


**Fig 1.4:** Mobile phones, Air traffic control, Directional drilling, Anomaly mapping.

- Use of electronic compasses now very widespead in mobile phones & compact cameras. Also for drill orientation in hydrocarbon industry.
- But requires an accurate model of the current geomagnetic field.
- Models become noticeably inaccurate within 5 years.

# A major scientific challenge

- **How can we better predict changes in Earth's magnetic field?**

# A major scientific challenge

- **How can we better predict changes in Earth's magnetic field?**

- Solution requires an improved knowledge and understanding of the 'weather' in Earth's core.

# A major scientific challenge

- **How can we better predict changes in Earth's magnetic field?**
- Solution requires an improved knowledge and understanding of the 'weather' in Earth's core.
- Strategies to attack this problem:

# A major scientific challenge

- **How can we better predict changes in Earth's magnetic field?**
- Solution requires an improved knowledge and understanding of the 'weather' in Earth's core.
- Strategies to attack this problem:
    - Re-analysis of past field evolution.

# A major scientific challenge

- **How can we better predict changes in Earth's magnetic field?**
- Solution requires an improved knowledge and understanding of the 'weather' in Earth's core.
- Strategies to attack this problem:
  - Re-analysis of past field evolution.
  - Higher resolution studies of present field evolution.

# A major scientific challenge

- **How can we better predict changes in Earth's magnetic field?**
- Solution requires an improved knowledge and understanding of the 'weather' in Earth's core.
- Strategies to attack this problem:
    - Re-analysis of past field evolution.
    - Higher resolution studies of present field evolution.
    - Development of new models of physics of Earth's core.

# Talk Outline

1. Introduction
2. Historical field evolution
3. Monitoring today's geodynamo
4. Origin of field changes: Dynamics of the core
5. Future prospects and conclusions

# History of studies in terrestrial magnetism I

- 1050 A.D. **Chinese scholars from Song Dynasty** note the use of magnets for navigational purposes.

# History of studies in terrestrial magnetism I

- 1050 A.D. **Chinese scholars from Song Dynasty** note the use of magnets for navigational purposes.

- 1269 **Petrus Peregerinus** carries out systematic experiments on properties of magnets.

# History of studies in terrestrial magnetism I

- 1050 A.D. **Chinese scholars from Song Dynasty** note the use of magnets for navigational purposes.
- 1269 **Petrus Peregerinus** carries out systematic experiments on properties of magnets.
- 1600 **William Gilbert** declares that Earth itself is a great magnet.

# William Gilbert: Physician and natural philosopher

**Fig 2.1:** William Gilbert, circa 1600.

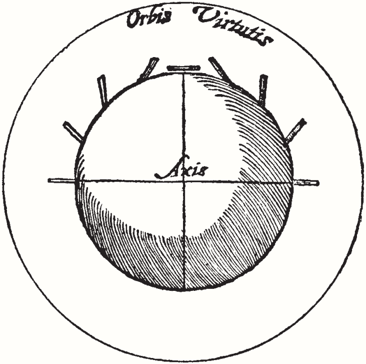


**Fig 2.2:** 'Orb Virbitus': Gilbert's term for sphere of influence surrounding a magnetic terella, from De Magnete, Book V, chapt. 2.

# History of studies in terrestrial magnetism I

- 1050 A.D. **Chinese scholars from Song Dynasty** note the use of magnets for navigational purposes.
- 1269 **Petrus Peregerinus** carries out systematic experiments on properties of magnets.
- 1600 **William Gilbert** declares that Earth itself is a great magnet.
- 1634 **Henry Gellibrand** discovers that Earth's magnetic field is slowly changing (secular variation).

# Historical Declination and Inclination in London

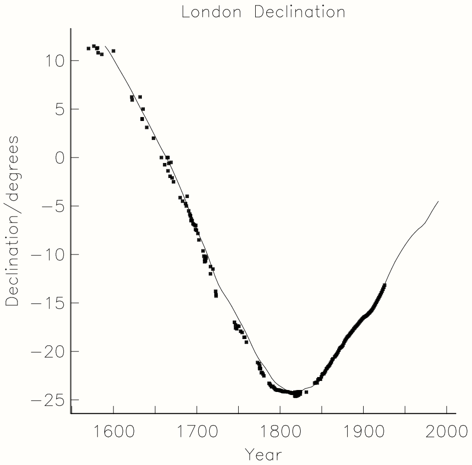


**Fig 2.3:** Changes of declination in London compared to *gufm1* model of Jackson et al. (2000).

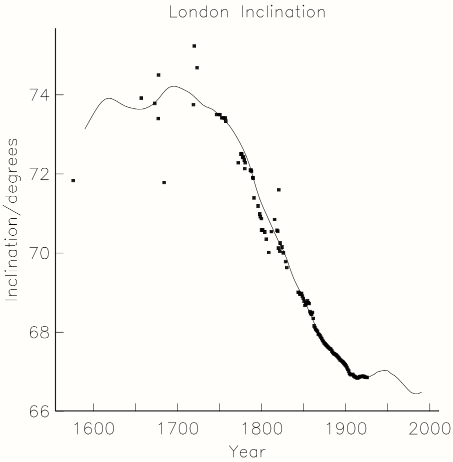


**Fig 2.4:** Changes of inclination in London compared to *gufm1* model of Jackson et al. (2000).

# History of studies in terrestrial magnetism II

- 1701 **Edmund Halley** presents a maps of declination derived from measurements he made during voyages in the Atlantic ocean.

# Edmund Halley: Geophysicist & Explorer


**Fig 2.5:** Edmund Halley in 1687 aged 32.


**Fig 2.6:** Halley's 1701 map of declination.

# History of studies in terrestrial magnetism II

- 1701 **Edmund Halley** presents a maps of declination derived from measurements he made during voyages in the Atlantic ocean.

- 1779 **James Cook** makes his final voyage of discovery to the Southern Seas, extensive magnetic observations made throughout.

# Captain James Cook: Voyages to Pacfic 1768-1779

**Fig 2.7:** Replica of Cook's Endeavour.

**Fig 2.8:** Captain James Cook in 1776, prior to his final voyage.

# Examples from mariner's logbooks

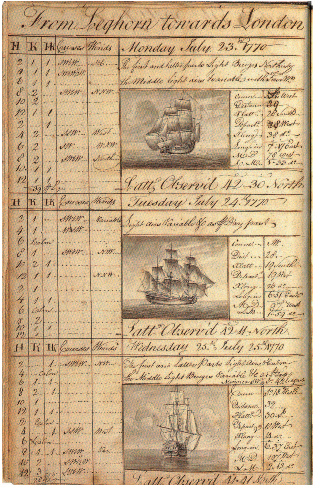


**Fig 2.9:** Extract from log book: From Leghorn to London, 23rd July 1770.

**Fig 2.10:** Illustration of a mariner determining $D$: Les premieres Oeuvres de Iacques de Vaulx, pilotte en la Marine (Havre de Grace 1583 (Credit: National Library, Paris).

- Log books from English, Dutch, French, Spanish and Danish mariners provide many thousands of valuable records.

# Geographic distribution of magnetic observations in the 18th century.

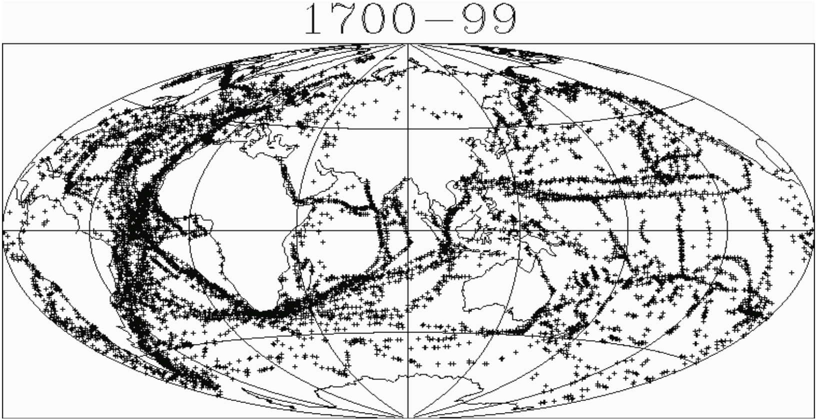


**Fig 2.11:** 18th century historical data distribution.

# History of studies in terrestrial magnetism II

- 1701 **Edmund Halley** presents a maps of declination derived from measurements he made during voyages in the Atlantic ocean.

- 1779 **James Cook** makes his final voyage of discovery to the Southern Seas, extensive magnetic observations made throughout.

- 1798 **Alexander von Humboldt** voyages to the Americas, carries out relative intensity experiments & shows field is weaker at low latitudes.

# Alexander Von Humboldt: Explorer and Polymath

**Fig 2.12:** Alexander von Humboldt circa 1806 after his return from American travels.


**Fig 2.13:** Humboldt's masterpiece 'Kosmos' (1846) was finally published in German, French and English.

# History of studies in terrestrial magnetism II

- 1701 **Edmund Halley** presents a maps of declination derived from measurements he made during voyages in the Atlantic ocean.

- 1779 **James Cook** makes his final voyage of discovery to the Southern Seas, extensive magnetic observations made throughout.

- 1798 **Alexander von Humboldt** voyages to the Americas, carries out relative intensity experiments & shows field is weaker at low latitudes.

- 1832 **Carl Friedrich Gauss** measures absolute intensity, promotes magnetic observatories and develops spherical harmonic analysis.

# Gauss, Weber and the Magnetic Union

**Fig 2.14:** Portrait of Gauss and Weber at the time of their collaboration in the study of geomagnetism.

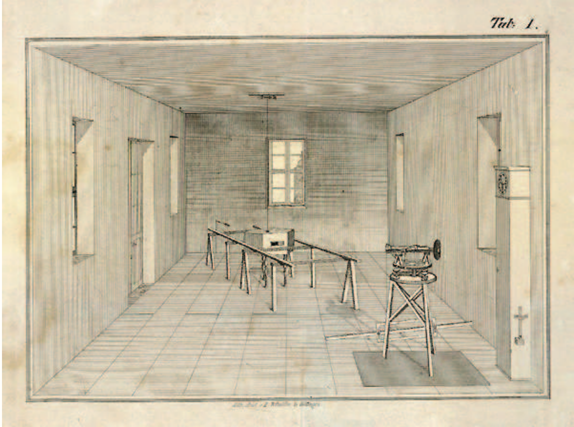


**Fig 2.15:** Inside Göttingen Magnetic Observatory, circa 1836.

# Temporal distribution of historical observations

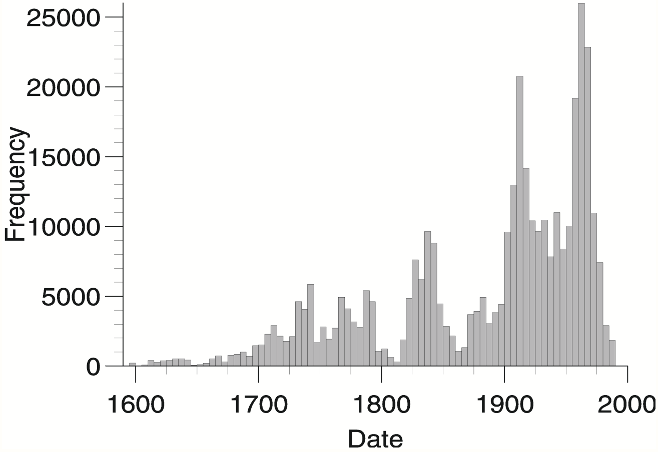


**Fig 2.16:** No. data versus time in 5 year bins from the *gufm1* model of Jackson et al. (2000).

# Change in declination over the past 400 years

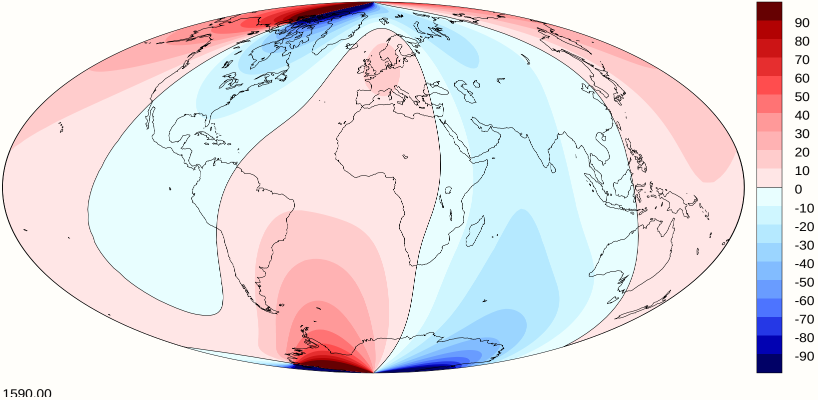


**Fig 2.17:** Declination at Earth's surface from 1590.0 to 1990.0 from the *gufm1 model of Jackson et al. (2000) : units* $\mu T$

# Change in radial field over past 400 years

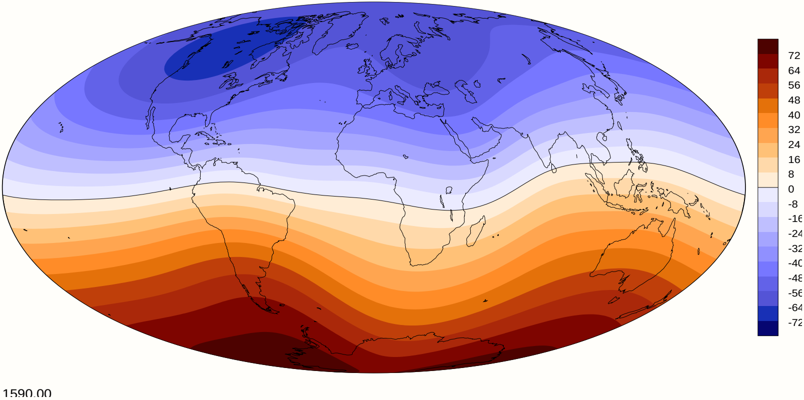


**Fig 2.18:** $B_r$ at Earth's surface from 1590.0 to 1990.0 from the *gufm1 model of Jackson et al. (2000) : units* $\mu T$

# Downward continuation of radial field to core surface

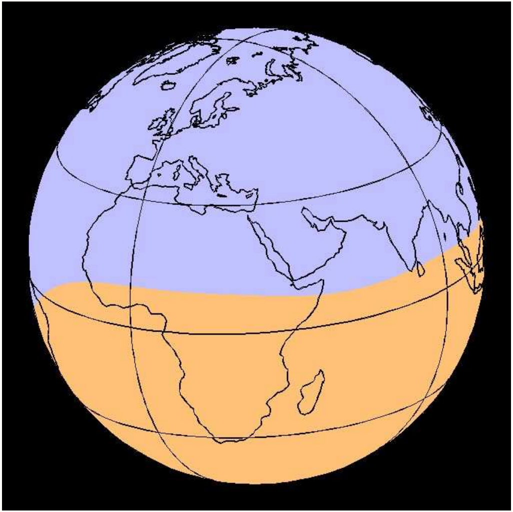

**Fig 2.19:** Change in $B_r$ during downward continuation (Credit: S. Gibbons)

# Evolution of radial field at the core surface

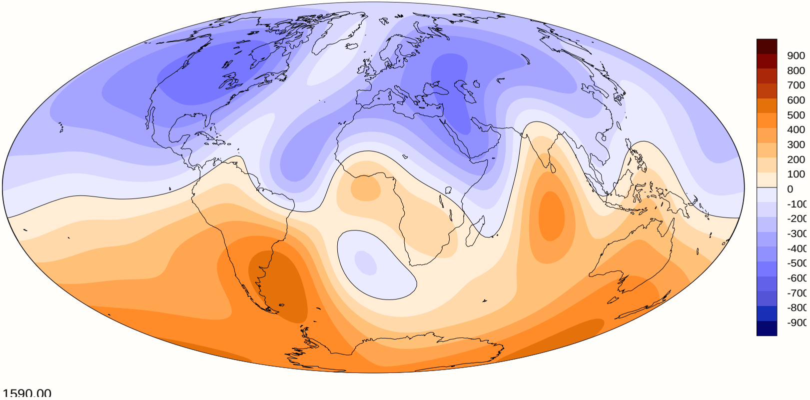


**Fig 2.20:** $B_r$ at core surface from 1590.0 to 1990.0 from the *gufm1 of* Jackson et al. (2000) *: units* $\mu T$

# Distribution of power for east-west motions

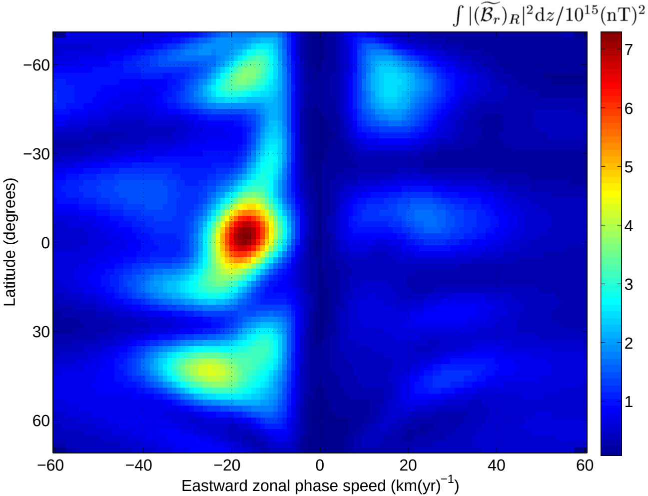


**Fig 2.21:** Power moving in the east-west diection as a function of latitude and azimuthal speed, from Radon transform of $B_r$ at core surface filtered to remove periods longer than 400 yrs. From Finlay & Jackson (2003).

# Time-Longitude analysis of field at equator

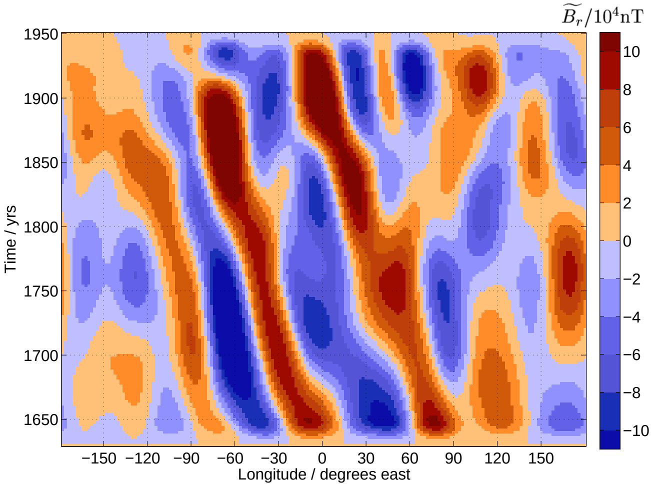


**Fig 2.22:** Historical evolution of radial magnetic field at core surface, filtered to remove changes with periods longer than 400 years. From Finlay & Jackson (2003).

# Summary of historical field evolution

- Dedication of individual observers over past four centuries has endowed us with a rich record of geomagnetic observations.

# Summary of historical field evolution

- Dedication of individual observers over past four centuries has endowed us with a rich record of geomagnetic observations.
- Earth's magnetic field has changed continuously over the past four centuries.

# Summary of historical field evolution

- Dedication of individual observers over past four centuries has endowed us with a rich record of geomagnetic observations.
- Earth's magnetic field has changed continuously over the past four centuries.
- Most striking feature at Earth's surface is westward drift.

# Summary of historical field evolution

- Dedication of individual observers over past four centuries has endowed us with a rich record of geomagnetic observations.
- Earth's magnetic field has changed continuously over the past four centuries.
- Most striking feature at Earth's surface is westward drift.
- More detail is revealed by downward continuing field to the surface of the core.

# Summary of historical field evolution

- Dedication of individual observers over past four centuries has endowed us with a rich record of geomagnetic observations.
- Earth's magnetic field has changed continuously over the past four centuries.
- Most striking feature at Earth's surface is westward drift.
- More detail is revealed by downward continuing field to the surface of the core.
- Westward drift is due to the motion of a series of field concentrations moving westwards under the Atlantic hemisphere.

# Talk Outline

1. Introduction
2. Historical field evolution
3. **Monitoring today's geodynamo**
4. Origin of field changes: Dynamics of the core
5. Future prospects and conclusions

# Modern monitoring of the geomagnetic field

- LEO Satellites: short term but excellent global coverage.

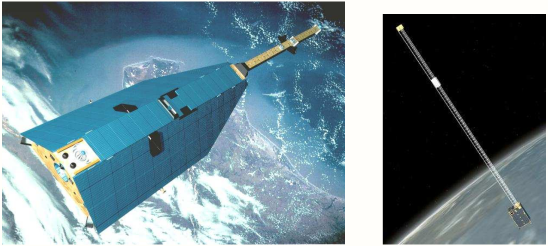

**Fig 3.1:** Satellites CHAMP (left) and Ørsted (right) measuring the geomagnetic field.

# Modern monitoring of the geomagnetic field

- LEO Satellites: short term but excellent global coverage.

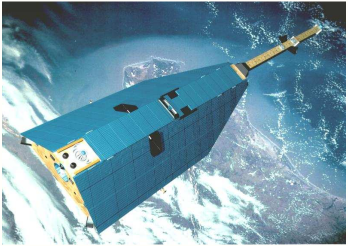
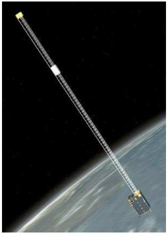

**Fig 3.1:** Satellites CHAMP (left) and Ørsted (right) measuring the geomagnetic field.

- High quality, long-term observations from worldwide network.


**Fig 4:** Brorfelde and Qeqertarsuaq/Godhavn observatories, operated by DTU Space.

# Observatory network

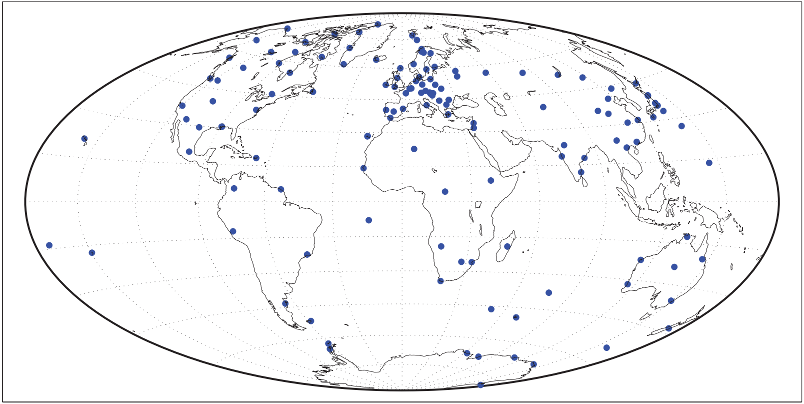

**Fig 3.3:** Locations of geomagnetic observatories providing data used for field modelling in the interval 2000-2010.

# Pre-processing of data

- Use CHAOS-3 (Olsen et al., 2010) dataset for 2000.0-2010.0.
- Sub-sample on equal area tessera reset every 0.25 yrs.
- Quiet time, night side, vector only $< |60 \text{ deg}|$ geomag lat.
- Subtract estimates of large scale magntospheric and crustal field.

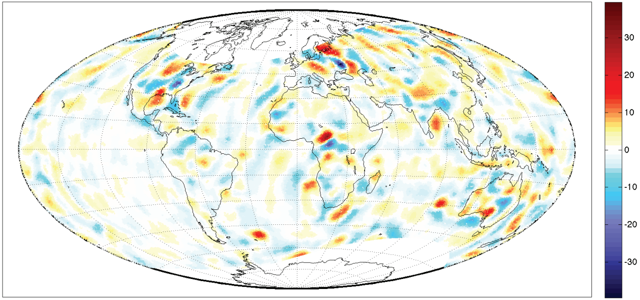


**Fig 3.4:** Map showing crustal corrections from model of Stockmann et al. (2009) applied to CHAMP vector $Z$ component data. Units are $nT$.

# Core field modelling

- Model core field as potential field with purely internal source,

$$\mathbf{B} = -\nabla V \qquad \text{and} \qquad \nabla \cdot \mathbf{B} = 0$$

$$\text{where} \quad V(r,\theta,\phi,t) = a\sum_{l=1}^{L}\sum_{m=0}^{l}\left(\frac{a}{r}\right)^{l+1} g_l^m(t)\,Y_l^m(\theta,\phi).$$

# Core field modelling

- Model core field as potential field with purely internal source,

$$\mathbf{B} = -\nabla V \qquad \text{and} \qquad \nabla \cdot \mathbf{B} = 0$$

$$\text{where} \quad V(r, \theta, \phi, t) = a \sum_{l=1}^{L} \sum_{m=0}^{l} \left(\frac{a}{r}\right)^{l+1} g_l^m(t) Y_l^m(\theta, \phi).$$

- Account for secular variation using a 6th-order B-spline basis for Gauss coefficients,

$$g_l^m(t) = \sum_n g_l^{mn} M_n(t).$$

# Core field modelling

- Model core field as potential field with purely internal source,

$$\mathbf{B} = -\nabla V \qquad \text{and} \qquad \nabla \cdot \mathbf{B} = 0$$

$$\text{where} \quad V(r,\theta,\phi,t) = a\sum_{l=1}^{L}\sum_{m=0}^{l}\left(\frac{a}{r}\right)^{l+1} g_l^m(t) Y_l^m(\theta,\phi).$$

- Account for secular variation using a 6th-order B-spline basis for Gauss coefficients,

$$g_l^m(t) = \sum_n g_l^{mn} M_n(t).$$

- Use SH expansion to degree L=24 and choose knot points every 0.25 yrs so that representation does not influence model.

# Core field modelling

- Model core field as potential field with purely internal source,

$$\mathbf{B} = -\nabla V \qquad \text{and} \qquad \nabla \cdot \mathbf{B} = 0$$

$$\text{where} \quad V(r,\theta,\phi,t) = a\sum_{l=1}^{L}\sum_{m=0}^{l}\left(\frac{a}{r}\right)^{l+1} g_l^m(t)Y_l^m(\theta,\phi).$$

- Account for secular variation using a 6th-order B-spline basis for Gauss coefficients,

$$g_l^m(t) = \sum_n g_l^{mn} M_n(t).$$

- Use SH expansion to degree L=24 and choose knot points every 0.25 yrs so that representation does not influence model.
- Solve inverse problem by minimizing a cost function: data misfit & a regularization norm based on core surface field,

$$\Theta = [\mathbf{d} - \mathbf{f}(\mathbf{m})]^T \mathbf{C}_e^{-1}[\mathbf{d} - \mathbf{f}(\mathbf{m})] + \mathcal{R}(\mathbf{m}).$$

$\mathcal{R}(\mathbf{m})$ is a norm measuring spatial & temporal complexity at CMB.

# Core field modelling II: Regularization

- The classic quadratic form of regularization is:

$$\mathcal{R}^{Q}(\mathbf{m}) = \frac{\lambda_S}{T_e - T_s} \int_{t_s}^{t_e} \int_{CMB} (B_r)^2 d\Omega\, dt + \frac{\lambda_T}{T_e - T_s} \int_{t_s}^{t_e} \int_{CMB} \left( \frac{\partial^3 B_r}{\partial t^3} \right)^2 d\Omega\, dt$$

# Core field modelling II: Regularization

- The classic quadratic form of regularization is:

$$\mathcal{R}^Q(\mathbf{m}) = \frac{\lambda_S}{T_e - T_s} \int_{t_s}^{t_e} \int_{CMB} (B_r)^2 d\Omega\, dt + \frac{\lambda_T}{T_e - T_s} \int_{t_s}^{t_e} \int_{CMB} \left( \frac{\partial^3 B_r}{\partial t^3} \right)^2 d\Omega\, dt$$

- Here we also investigate models constructed using 'entropy' regularization in space (Jackson et al., 2007a; Gillet et al., 2007):

$$\mathcal{R}^E(\mathbf{m}) = \frac{\lambda_S}{T_e - T_s} \int_{t_s}^{t_e} \int_{CMB} S(B_r) d\Omega\, dt + \frac{\lambda_T}{T_e - T_s} \int_{t_s}^{t_e} \int_{CMB} \left( \frac{\partial^3 B_r}{\partial t^3} \right)^2 d\Omega\, dt$$

where $\quad S(x) = -4d \left( \Psi - 2d - x \ln \left[ \frac{\Psi + x}{2d} \right] \right) \quad$ with $\quad \Psi = \sqrt{x^2 + 4d^2}$

$-S(x)$ is a generalized (normalized, co-ordinate invariant) form of the configuration entropy (Sivia & Skilling, 2006) that applies to scalar functions that may be either positive and negative.

# Fit to satellite data : CHAMP Z component

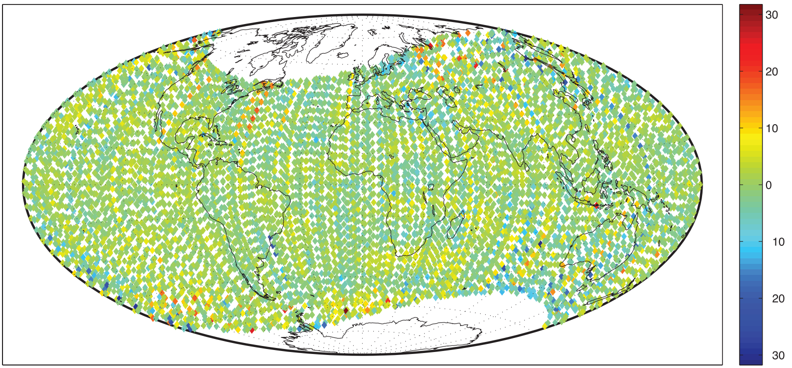


**Fig 3.5:** Residuals between field model and CHAMP vector data (Z component) in 2008. Units are $nT$.

# Fit to observatory data : Z component

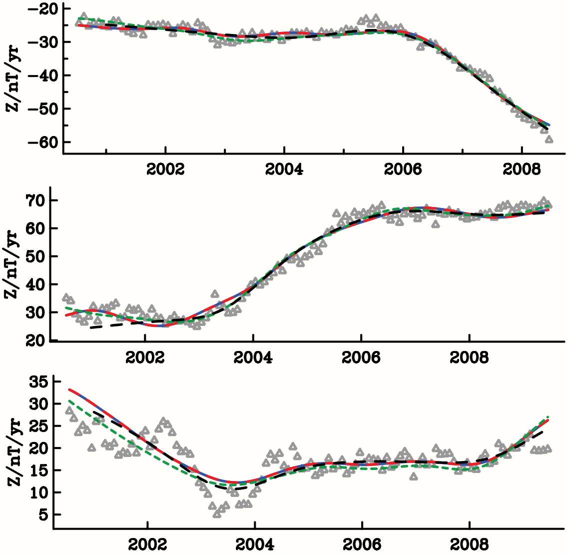


**Fig 3.6:** Comparison of $Y$ at Earth's surface with annual differences of month means in grey triangles at HUA, LRM and GUA, red/blue is our model, black dashed is CHAOS-3, green dashed is GRIMM2.

# Core surface field evolution 2000 - 2010

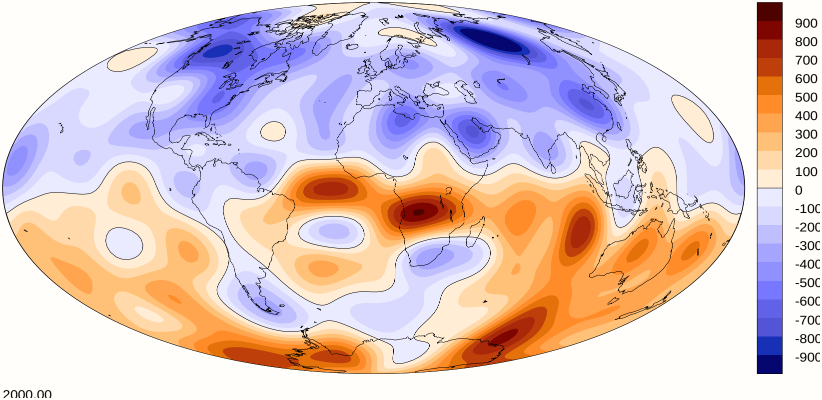


**Fig 3.7:** $B_r$ at core surface from 2000.0 to 2010.0 : units $\mu$T

# Core surface field acceleration 2000 - 2010


**Fig 3.8 :** Second time derivative of $B_r$ at core surface from 2000.0 to 2010.0: units $\mu$T/yr$^2$

# Summary of present field evolution

- Satellite and observatory data provide excellent spatial coverage and good temporal constraints on core field evolution.

# Summary of present field evolution

- Satellite and observatory data provide excellent spatial coverage and good temporal constraints on core field evolution.
- Maps of the core surface field display intense concentrations at low latitude which are rapidly evolving.

# Summary of present field evolution

- Satellite and observatory data provide excellent spatial coverage and good temporal constraints on core field evolution.
- Maps of the core surface field display intense concentrations at low latitude which are rapidly evolving.
- Efforts to predict future secular variation need to be capable of modelling these features.

# Talk Outline

# Ingredients of core dynamics

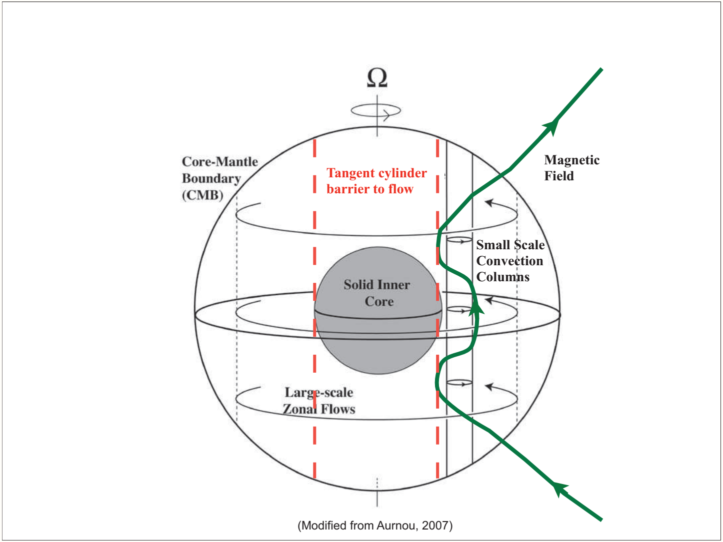


**Fig 4.1:** Schematic picture showing key ingredients of core dynamics.

# Governing equations

# Governing equations

- $$Ro\left(\frac{\partial \mathbf{u}}{\partial t}+\mathbf{u}.\nabla\mathbf{u}\right)+\boldsymbol{\Omega}\times\mathbf{u}=-\nabla p-qRaT\,\mathbf{g}+(\nabla\times\mathbf{B})\times\mathbf{B}+E\nabla^2\mathbf{u}$$

# Governing equations

- $$Ro\left(\frac{\partial \mathbf{u}}{\partial t}+\mathbf{u}.\nabla\mathbf{u}\right)+\boldsymbol{\Omega}\times\mathbf{u}=-\nabla p-qRaT\,\mathbf{g}+(\nabla\times\mathbf{B})\times\mathbf{B}+E\nabla^2\mathbf{u}$$
- $$\frac{\partial \mathbf{B}}{\partial t}=\nabla\times(\mathbf{u}\times\mathbf{B})+\nabla^2\mathbf{B}$$

# Governing equations

- $$Ro\left(\frac{\partial \mathbf{u}}{\partial t} + \mathbf{u}.\nabla\mathbf{u}\right) + \boldsymbol{\Omega}\times\mathbf{u} = -\nabla p - qRaT\,\mathbf{g} + (\nabla\times\mathbf{B})\times\mathbf{B} + E\nabla^2\mathbf{u}$$
- $$\frac{\partial \mathbf{B}}{\partial t} = \nabla\times(\mathbf{u}\times\mathbf{B}) + \nabla^2\mathbf{B}$$
- $$\frac{\partial T}{\partial t} + \mathbf{u}\cdot\nabla T = q\nabla^2 T$$

# Governing equations

- $$Ro\left(\frac{\partial \mathbf{u}}{\partial t} + \mathbf{u}.\nabla\mathbf{u}\right) + \mathbf{\Omega}\times\mathbf{u} = -\nabla p - qRaT\,\mathbf{g} + (\nabla\times\mathbf{B})\times\mathbf{B} + E\nabla^2\mathbf{u}$$
- $$\frac{\partial \mathbf{B}}{\partial t} = \nabla\times(\mathbf{u}\times\mathbf{B}) + \nabla^2\mathbf{B}$$
- $$\frac{\partial T}{\partial t} + \mathbf{u}\cdot\nabla T = q\nabla^2 T$$
- $$Ro = \frac{\eta}{2\Omega r_o^2} \qquad Ra = \frac{g_0\alpha\beta r_o^2}{2\Omega\kappa} \qquad E = \frac{\nu}{2\Omega r_o^2} \qquad q = \frac{\kappa}{\eta}$$

# Governing equations

- $$Ro\left(\frac{\partial \mathbf{u}}{\partial t} + \mathbf{u}.\nabla\mathbf{u}\right) + \boldsymbol{\Omega}\times\mathbf{u} = -\nabla p - qRaT\,\mathbf{g} + (\nabla\times\mathbf{B})\times\mathbf{B} + E\nabla^2\mathbf{u}$$
- $$\frac{\partial \mathbf{B}}{\partial t} = \nabla\times(\mathbf{u}\times\mathbf{B}) + \nabla^2\mathbf{B}$$
- $$\frac{\partial T}{\partial t} + \mathbf{u}\cdot\nabla T = q\nabla^2 T$$
- $$Ro = \frac{\eta}{2\Omega r_o^2} \qquad Ra = \frac{g_0\alpha\beta r_o^2}{2\Omega\kappa} \qquad E = \frac{\nu}{2\Omega r_o^2} \qquad q = \frac{\kappa}{\eta}$$
- **Earth** : $Ro = 10^{-9}$ $\qquad Ra \sim 10^{15}$ $\qquad E = 10^{-15}$ $\qquad q = 10^{-5}$

# Governing equations

- $$Ro\left(\frac{\partial \mathbf{u}}{\partial t} + \mathbf{u}.\nabla\mathbf{u}\right) + \boldsymbol{\Omega}\times\mathbf{u} = -\nabla p - qRaT\,\mathbf{g} + (\nabla\times\mathbf{B})\times\mathbf{B} + E\nabla^2\mathbf{u}$$
- $$\frac{\partial \mathbf{B}}{\partial t} = \nabla\times(\mathbf{u}\times\mathbf{B}) + \nabla^2\mathbf{B}$$
- $$\frac{\partial T}{\partial t} + \mathbf{u}\cdot\nabla T = q\nabla^2 T$$
- $$Ro = \frac{\eta}{2\Omega r_o^2} \qquad Ra = \frac{g_0\alpha\beta r_o^2}{2\Omega\kappa} \qquad E = \frac{\nu}{2\Omega r_o^2} \qquad q = \frac{\kappa}{\eta}$$
- $$\textbf{Earth}: \quad Ro = 10^{-9} \qquad Ra \sim 10^{15} \qquad E = 10^{-15} \qquad q = 10^{-5}$$
- Difficulties:
  - (i) Coupled nonlinear system.
  - (ii) Large disparities of time scales and lenth scales.

# Approach 1: Direct Numerical Simulation

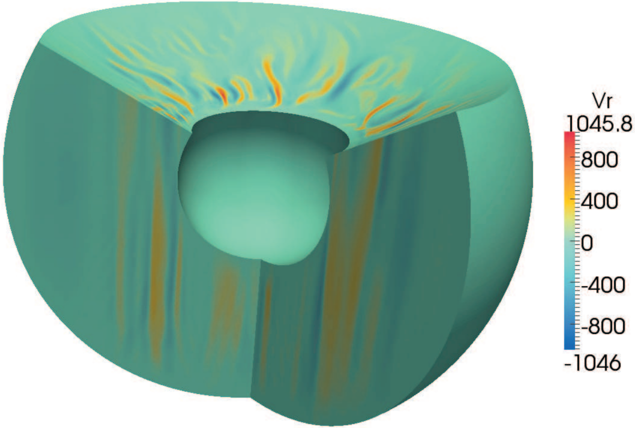


**Fig 4.1:** Radial component of flow inside 3D spherical shell simulation with Ro=$10^{-6}$, E=$10^{-6}$, Ra=$3.10^3$, q=1. (Courtesy of Andrey Sheyko - ETHZ PhD Student).

# Approach 1: Direct Numerical Simulation

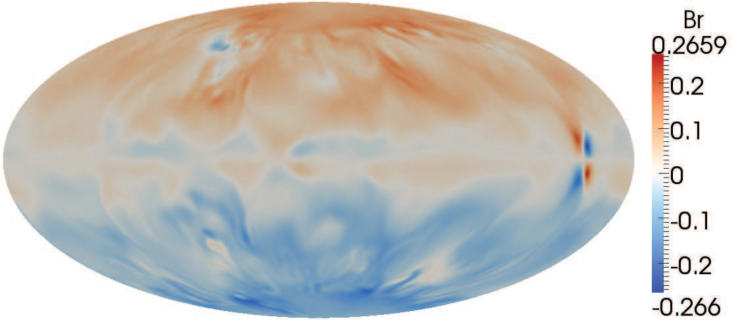


**Fig 4.2:** Radial magnetic field at outer bounary of 3D spherical shell simulation with Ro=$10^{-6}$, E=$10^{-6}$, Ra=$3.10^{3}$, q=1. (Courtesy of Andrey Sheyko - ETHZ PhD Student)

# Approach 2: Simplified model

- Neglect small inertial & viscous terms & assume that convective driving appears at higher order to drive motions against weak magnetic dissipation (Zhang, 1994; Zhang et al., 2003).

# Approach 2: Simplified model

- Neglect small inertial & viscous terms & assume that convective driving appears at higher order to drive motions against weak magnetic dissipation (Zhang, 1994; Zhang et al., 2003).

- $$\boldsymbol{\Omega} \times \mathbf{u} = -\nabla p + (\nabla \times \mathbf{B}) \times \mathbf{B}$$
  $$\frac{\partial \mathbf{B}}{\partial t} = \nabla \times (\mathbf{u} \times \mathbf{B})$$

# Approach 2: Simplified model

- Neglect small inertial & viscous terms & assume that convective driving appears at higher order to drive motions against weak magnetic dissipation (Zhang, 1994; Zhang et al., 2003).

- $$\boldsymbol{\Omega} \times \mathbf{u} = -\nabla p + (\nabla \times \mathbf{B}) \times \mathbf{B}$$
$$\frac{\partial \mathbf{B}}{\partial t} = \nabla \times (\mathbf{u} \times \mathbf{B})$$

- These equations may be linearized, combined into a single wave equation, and then solved subject to no penetration and insulating BC to obtain normal modes.

# Simplified model of rotating flows

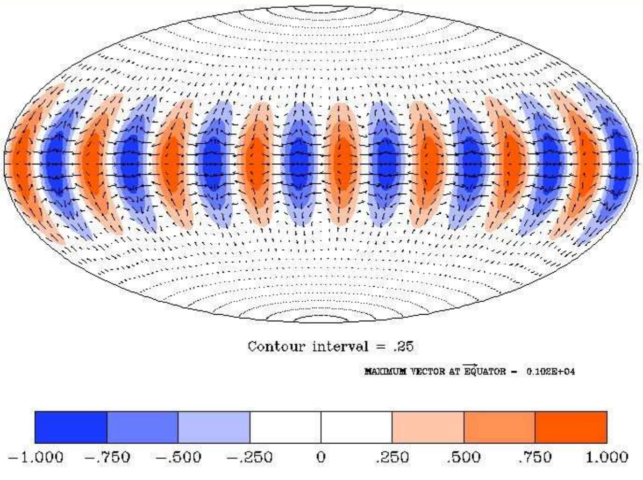


**Fig 4.3:** Example normal mode of rotating MHD flow close to the core surface, orange denotes upwelling, blue denotes downwelling.

# Synthetic field evolution produce by wave flow

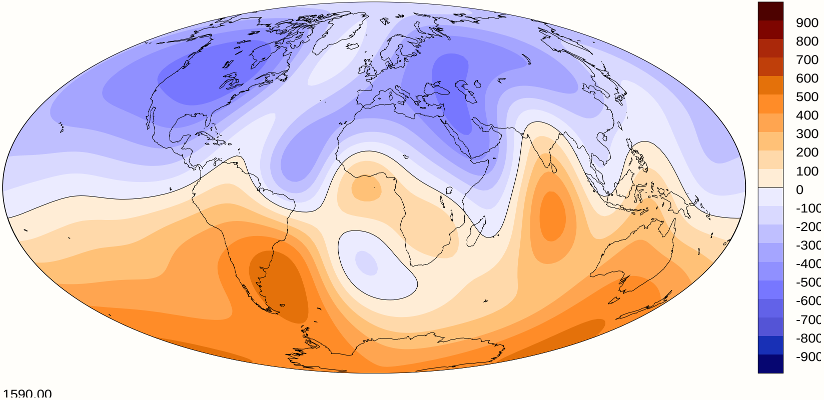


**Fig 4.4:** Synthetic $B_r$ at core surface from 1590.0 to 1990.0 using simple wave flow acting on 1590 initial field : units $\mu$T. From Finlay (2005).

# Summary of theory of secular variation

- Equations governing convection-driven, rotating MHD are difficult to solve in the parameter regime expected in Earth's core.

# Summary of theory of secular variation

- Equations governing convection-driven, rotating MHD are difficult to solve in the parameter regime expected in Earth's core.

- Nonetheless, much progress has been made in the past 15 yrs using supercomputers to produce dipole-dominated dynamo simulations, but understanding of rapid secular variation remains elusive.

# Summary of theory of secular variation

- Equations governing convection-driven, rotating MHD are difficult to solve in the parameter regime expected in Earth's core.
- Nonetheless, much progress has been made in the past 15 yrs using supercomputers to produce dipole-dominated dynamo simulations, but understanding of rapid secular variation remains elusive.
- An alternative approach is to pursue simple models of the essential physics. Promising results are obtained with simple wave models.

# Summary of theory of secular variation

- Equations governing convection-driven, rotating MHD are difficult to solve in the parameter regime expected in Earth's core.

- Nonetheless, much progress has been made in the past 15 yrs using supercomputers to produce dipole-dominated dynamo simulations, but understanding of rapid secular variation remains elusive.

- An alternative approach is to pursue simple models of the essential physics. Promising results are obtained with simple wave models.

- Now need to make use of observations to better constrain physical models and to test their predictive ability.

# Talk Outline

1. Introduction
2. Historical field evolution
3. Monitoring today's geodynamo
4. Origin of field changes: Dynamics of the core
5. **Future prospects and conclusions**

# SWARM and assimilation into dynamical models

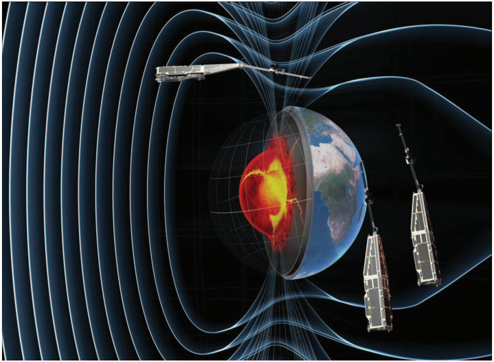

**Fig 5.1:** Visualization of SWARM: ESA Earth Observation constellation. (picture credit: ESA).

- SWARM will provide essential high quality data in upcoming years.
- Need to develop framework to encorporate satellite data into dynamical models (e.g. Dedicated data selection and processing, error covariance models, assimilation schemes).

# Extending the empirical record further back in time

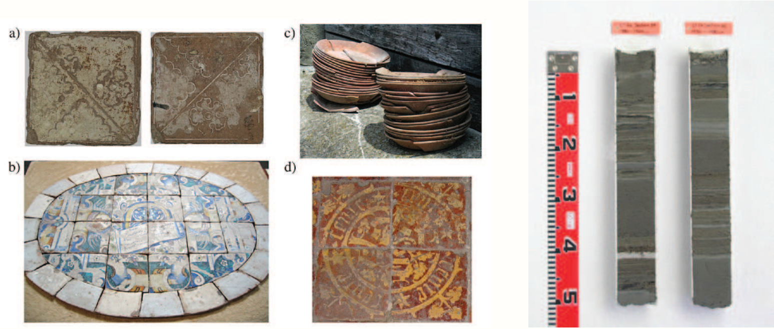


**Fig 5.2:** Left: Example of artefacts used in archeomagnetic samping (Genevey et al., 2009); Right: Example of a lake sediment core.

- Archeomagnetic and lake sediment records could provide long term constraints.
- Modelling perhaps requires probabilistic approach with spatially and temporally correlated priors.

# Conclusions

# Conclusions

- Historical observations reveal that westward motion of low latitude flux concentrations is an important component of geomagnetic secular variation.

# Conclusions

- Historical observations reveal that westward motion of low latitude flux concentrations is an important component of geomagnetic secular variation.
- Recent observations show that low latitude flux concentrations are very intense and that they are evolving rapidly.

# Conclusions

- Historical observations reveal that westward motion of low latitude flux concentrations is an important component of geomagnetic secular variation.
- Recent observations show that low latitude flux concentrations are very intense and that they are evolving rapidly.
- Improved predictions of the geomagnetic secular variation will require that the dynamics of such features is adequately modelled.

# Conclusions

- Historical observations reveal that westward motion of low latitude flux concentrations is an important component of geomagnetic secular variation.
- Recent observations show that low latitude flux concentrations are very intense and that they are evolving rapidly.
- Improved predictions of the geomagnetic secular variation will require that the dynamics of such features is adequately modelled.
- Assimilation of satellite data into dynamical models appears to be promising avenue for future progress.

Finlay, C. C., 2005. *Hydromagnetic waves in Earth's core and their influence on geomagnetic secular variation*, Ph.D Thesis, University of Leeds.

Finlay, C. C. & Jackson, A., 2003. Equatorially dominated magnetic field change at the surface of Earth's core, *Science*, **300**, 2084–2086.

Finlay, C. C., Maus, S., Beggan, C., Hamoudi, M., Lowes, F. J., Olsen, N., & Thébault, E., 2010. Evaluation of candidate geomagnetic field models for IGRF-11, *Earth, Planets, Space*, p. (submitted to EPS).

Genevey, A., Gallet, Y., Rosen, J., & LeGoff, M., 2009. Evidence for rapid geomagnetic !eld intensity variations in western europe over the past 800 years from new french archeointensity data, *Earth Planet. Sci. Lett.*, pp. 132–143.

Gillet, N., Jackson, A., & Finlay, C. C., 2007. Maximum entropy regularization of time-dependent geomagnetic field models, *Geophys. J. Int.*, **171**, 1005–1016.

Jackson, A., Jonkers, A. R. T., & Walker, M. R., 2000. Four centuries of geomagnetic secular variation from historical records, *Phil. Trans. R. Soc. Lond. A*, **358**, 957–990.

Jackson, A., Constable, C., & Gillet, N., 2007a. Maximum entropy regularization of the geomagnetic core field inverse problem, *Geophys. J. Int.*, **171**, 995–1004.

Jaynes, E. T., 1957. Information theory and statistical mechanics, *Phys. Rev. Lett.*, **106(4)**, 620–630.

Jonkers, A. R. T., 2003. *Earth's Magnetism in the Age of Sail*, Johns Hopkins Univeristy Press.

Maus, S., Macmillan, S., Chernova, T., Choi, S., Dater, D., Golovkov, V., Lesur, V., Lowes, F., Lühr, H., Mai, W., McLean, S., Olsen, N., Rother, M., Sabaka, T., Thomson, A., & Zvereva, T., 2005. The 10th-Generation International Geomagnetic Reference Field., *Geophys. J. Int.*, **161**, 561–565.

Olsen, N., Lühr, H., Mandea, M., Sabaka, T. J., & Tø ffner Clausen, L., 2010. The CHAOS-3 geomagnetic field model and candidate models for igrf-2010, p. in press.

Sivia, D. & Skilling, J., 2006. *Data Analysis: A Bayesian Tutorial*, Oxford University Press.

Stockmann, R., Finlay, C., & Jackson, A., 2009. Imaging earth's crustal magnetic field with satellite data: a regularized spherical triangle tessellation approach, *Geophys. J. Int.*, **179**, 929–944.

Zhang, K., 1994. On coupling between the poincare equation and the heat equation, *J. Fluid Mech.*, **268**, 211–229.

Zhang, K., Liao, X., & Schubert, G., 2003. Non-axisymmetric instabilities of a torioidal magnetic field in a rotating sphere, *Astr. J.*, **585**, 1124–1137.

# Failure of current IGRF predictions

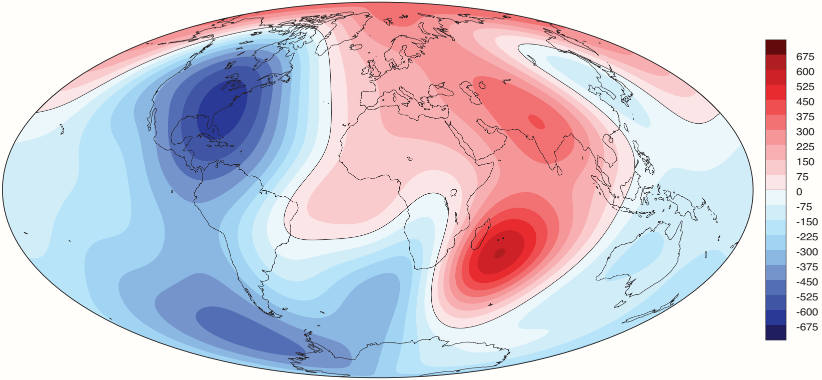


**Fig 0.1:** Error in field intensity in 2010 predicted by IGRF-10 (Maus et al., 2005) compared to IGRF-11 (Finlay et al., 2010) in 2010. Units are nT.

# Accuracy of maritime declination measurements

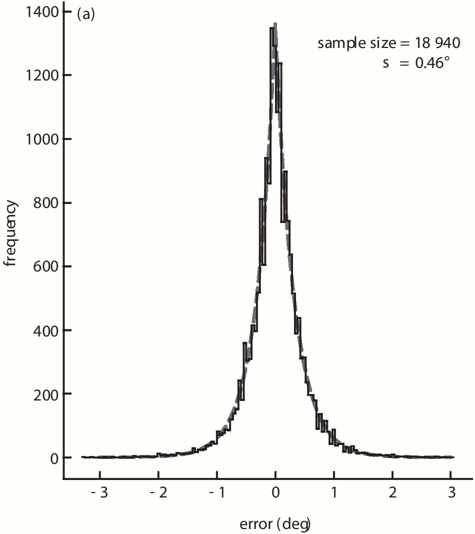


**Fig 0.2:** Distribution of deviations of Declination measurments from daily mean, when more than one measurement taken on a certain day. From Jackson et al. (2000)

# Determination of declination by mariners

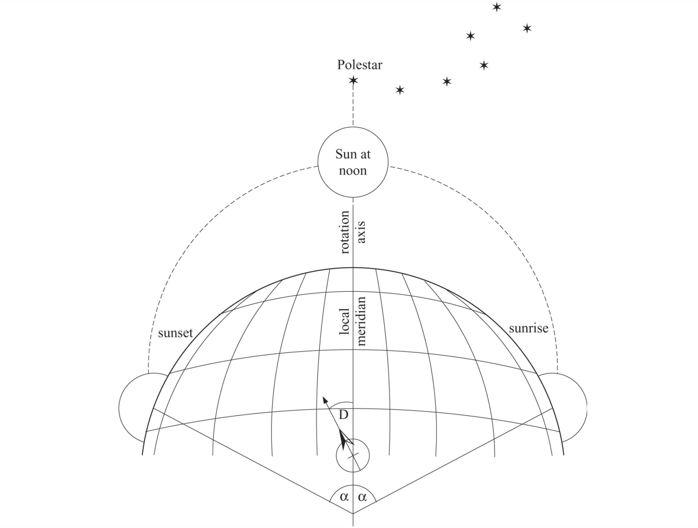


**Fig 0.3:** Determinations of declination by mariners. From Jonkers (2003).

# Core field modelling I: Sampling the CMB field

- Observations at surface and satellite altitude depend on weighted average of core field; for example:

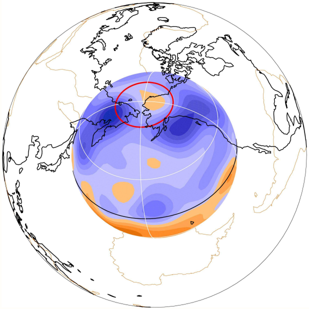

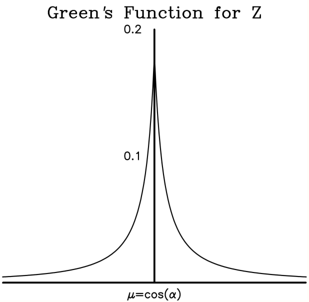


**Fig 0.4:** Z at core surface with Earth's surface shown together with the relevant Green's fns.

- We seek simple (minimum norm), converged, core surface fields that can account for observations within estimated errors.

# Core field modelling: Entropy regularization

- Jaynes (1957) set out the rationale for using maximum entropy to allocate probabilities in the absence of other information:
- "the maximum-entropy estimate ... is the least biased estimate possible on the given information; i.e. it is maximally non-committal with regard to missing information"
- Often applied to reconstruction of images from incomplete and noisy data e.g.in astronomy, image processing and medical tomography.
- **In Geomagnetism:**

  (i) Assumes there is a finite amount of magnetic flux.
  (ii) All possible arrangements assumed equally likely before the data arrives.
  (iii) Consideration of all possible combinations => $x \ln x$ factor.

# Core field modelling: Entropy regularization (cont)

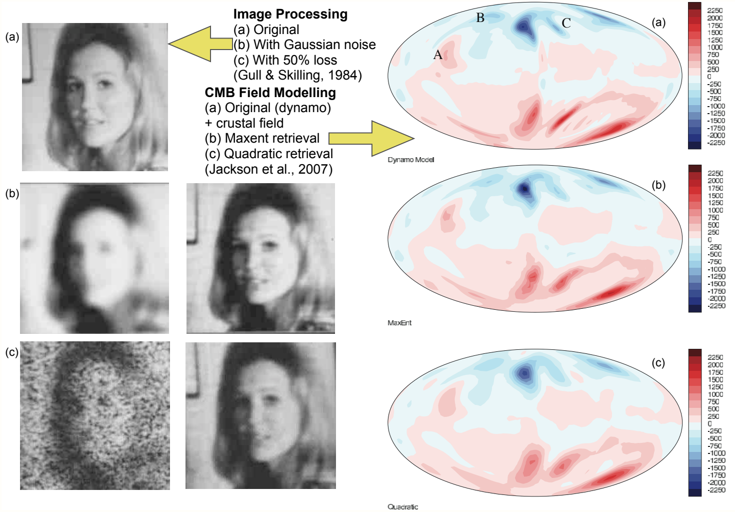


- Entropy regularisation performs well many in deconvolution problems and produces a simple solution without penalizing dynamic range.

# Temporal distribution of observations 2000-2010

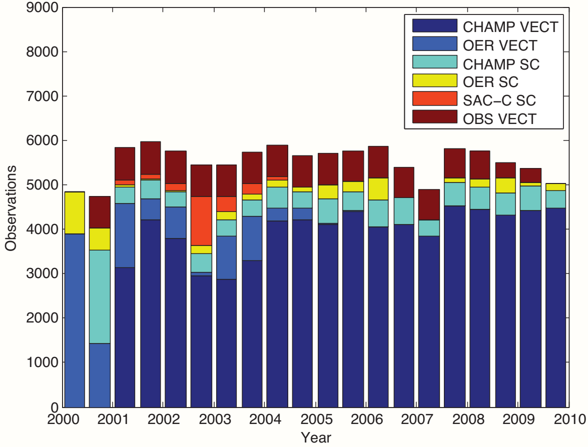


**Fig 0.5:** Temporal distribution of data types used to construct a field model of the past decade. Vector measurments are counted as a single observation.

# Fit to satellite data II

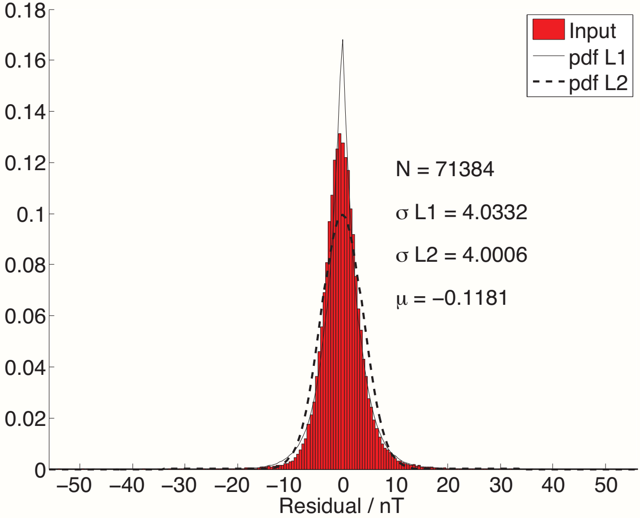


**Fig 0.6:** Histogram of residuals between field model and all CHAMP Z component data.

# Fit to observatory data II: Y component

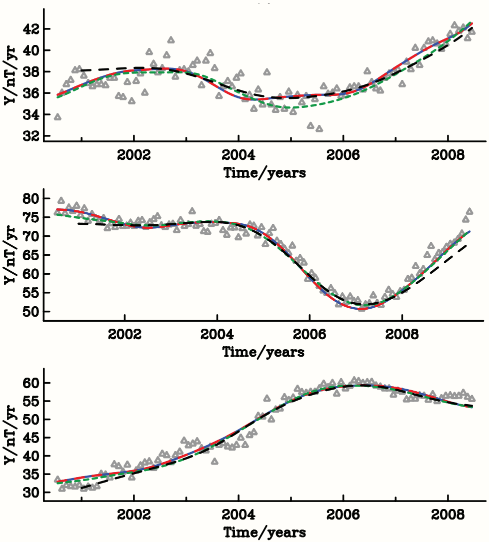


**Fig 0.7 :** Comparison of $Y$ at Earth's surface with annual differences of month means (black triangles) at BFE, MBO and AMS, red/blue is our model, black dashed is CHAOS-3, green dashed is GRIMM2.

# MF Spectra

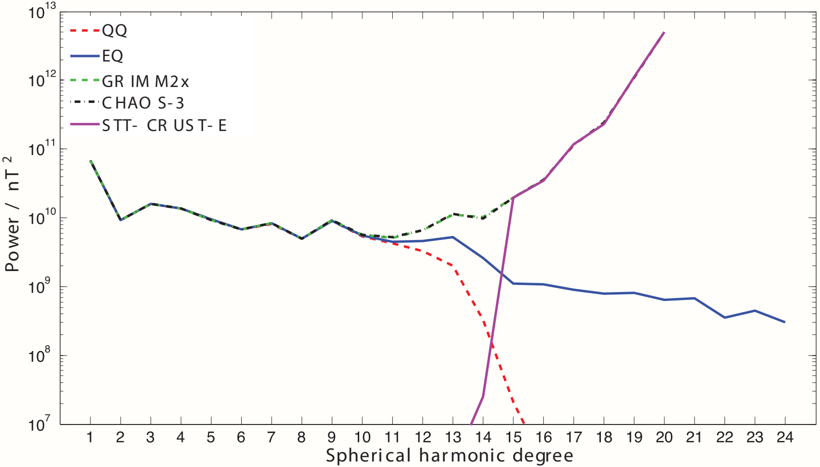


**Fig 0.8:** Comparison of MF spectra..

# SV Spectra

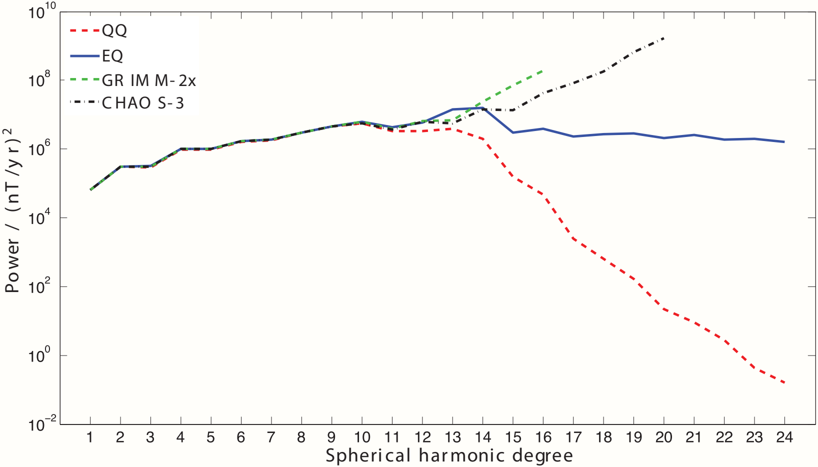


**Fig 0.9:** Comparison of SV spectra.

# SA Spectra

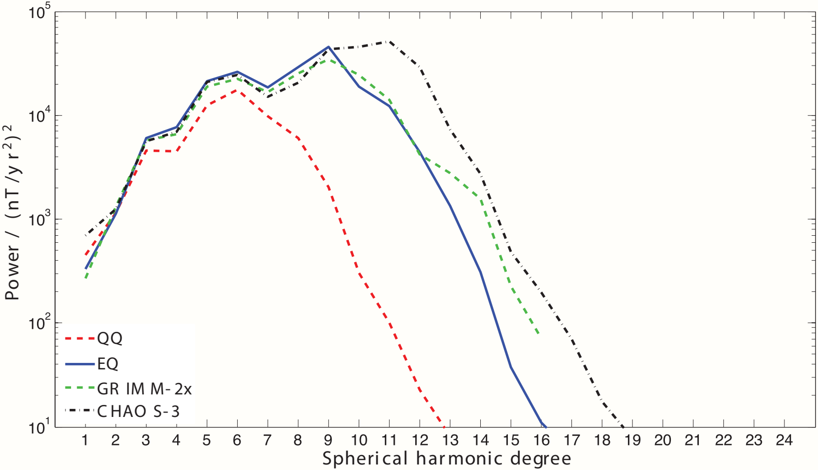


**Fig 0.10:** Comparison of SA spectra.